Iterative tuning of feedforward IPC for two-bladed wind turbines

Mulders, Sebastiaan; van Solingen, Edwin; van Wingerden, Jan-Willem; Beerens, J

DOI
10.1088/1742-6596/753/5/052027

Publication date
2016

Document Version
Final published version

Published in
Journal of Physics: Conference Series

Iterative tuning of feedforward IPC for two-bladed wind turbines

SP Mulders[1], E van Solingen[1], JW van Wingerden[1] and J Beerens[2]

[1]: Delft Center for Systems and Control, Faculty of Mechanical Engineering, Delft University of Technology, Mekelweg 2, 2628 CD Delft, The Netherlands

[2]: 2-B Energy BV, Welbergweg 54, 7556 PE Hengelo, The Netherlands, +31 (0)74 256 6330, www.2-benergy.com

E-mail: s.p.mulders@tudelft.nl

Abstract. At present, the cost of offshore wind energy does not meet the level of onshore wind and fossil-based energy sources. One way to extend the turbine lifetime, and thus reduce cost, is by reduction of the fatigue loads of blades and other turbine parts using Individual Pitch Control (IPC). This type of control, which is generally implemented by feedback control using the Multi-Blade Coordinate transformation on blade load measurement signals, is capable of mitigating the most dominant periodic loads. The main goal of this article is to develop a self-optimizing feedforward IPC strategy for a two-bladed wind turbine to reduce actuator duty cycle and reduce the dependency on blade load measurement signals. The approach uses blade load measurement data only initially for tuning of the feedforward controller, which is scheduled on the rotor azimuth angle and wind speed. The feedforward strategy will be compared to the feedback implementation in terms of load alleviation capabilities and actuator duty cycle. Results show that the implementation is capable of learning the optimal feedforward IPC controller in constant and turbulent wind conditions, to alleviate the pitch actuator duty cycle, and to considerably reduce harmonic fatigue loads without the need for blade load measurement signals after tuning.

1. Introduction

Wind energy is nowadays an important contributing energy source and is seen as an opportunity towards sustainable energy production because of its high power generation capabilities, scalability and possibility for deployment at offshore locations. With the increasing desire to deploy wind turbines at offshore locations combined with the higher cost, the focus is mainly set on the reduction of the Levelized Cost of Energy (LCOE) of offshore wind turbines [1]. In an attempt to lower the LCOE of offshore wind, a variety of approaches have been initiated, such as the development of larger multi-megawatt wind turbines, two-bladed offshore wind turbines [2], and wind turbines with a hydraulic transmission system [3]. Lowering costs can also be attained with control by reducing fatigue loads on different turbine components using pitch. In contrast to the ability of only collectively pitching the blades for speed regulation in the above-rated region, blades can be individually pitched in a number of recent wind turbines [4]. Individually pitching the blades by Individual Pitch Control (IPC) enables to significantly lower fatigue loads on the blades and other turbine components [5], resulting in an extended lifetime and a reduced LCOE.

Individual Pitch Control is generally implemented with use of the Multi-Blade Coordinate (MBC) transformation [6, 7], also referred to as the Coleman/Fourier coordinate transformation

in helicopter theory [8], or the direct-quadrature-zero (dq0) transformation in electrical machine theory [9]. The MBC transformation uses blade load and rotor azimuth measurement signals in a feedback control scheme, and transforms them from a rotating into a non-rotating reference frame and decouples the signals in a tilt and yaw component, which makes Single-Input Single-Output (SISO) control design possible [10]. The feedback IPC implementation is generally tested and tuned on a model of the wind turbine, and because of differences between the model and actual system dynamics, the IPC controller is likely to perform suboptimal on the real-world system.

One way to overcome the above mentioned problem, is by constructing the controller on identified disturbance and plant models. This approach applied for wind turbine load control is described in [11], where Repetitive Control (RC) is combined with subspace identification to form an adaptive control law for periodic disturbances, called Subspace Predictive Repetitive Control (SPRC). However, this method still depends on the availability of blade load measurement signals to identify system models.

Moreover, controllers are generally designed on Linear Time-Invariant (LTI) models obtained by linearization of physical models or system identification. A method that optimizes parameterized fixed-structure controllers online (on the actual system) in a closed-loop fashion is Iterative Feedback Tuning (IFT). This method does not require a model and overcomes the previously mentioned problem of model-plant mismatch. With IFT, the controller parameters are iteratively updated by obtaining the gradient of a predefined cost function with respect to the controller parameters by means of closed-loop experiments [12, 13, 14]. IFT has been implemented successfully on an actual system for temperature regulation in a distillation column [12] and more recently on wind turbine controllers for optimization of collective pitch and drive-train damping control [15].

The contribution of this paper is the implementation and optimization of a fixed-structure feedforward IPC controller. The feedforward controller is scheduled on the rotor azimuth and a wind speed estimate or measurement, and is optimized by an iterative procedure based on the ideas behind IFT. The feedforward controller is aimed to minimize for 1P and 2P blade loads. The algorithm optimization performance will be compared for constant and turbulent wind conditions. Furthermore, blade load reduction capabilities and the actuator duty cycle will be compared to the conventional feedback IPC approach.

This paper is organized as follows. In the next section, the theory behind and the implementation of the algorithm is explained. Subsequently, in Section 3, results of the optimization process and a performance comparison of the feedforward IPC implementation to the cases with feedback IPC and without IPC are given. Finally, conclusions are drawn in Section 4.

2. Theory and implementation

On the basis of the ideas behind IFT, a fixed-structure feedforward IPC controller, scheduled on the rotor azimuth position and a wind speed estimate or measurement, is implemented and optimized on blade load measurement signals by an iterative procedure. In this paper, the feedback case of the IFT optimization algorithm will not be considered, and the interested reader is referred to [12, 16, 17] for theoretical background and applications. The feedforward controller optimization can be performed initially for controller synthesis, and periodically to adapt to changed system characteristics and environmental conditions, but does not run continuously. For this reason, blade load measurements are not a critical part of the feedfoward control im-

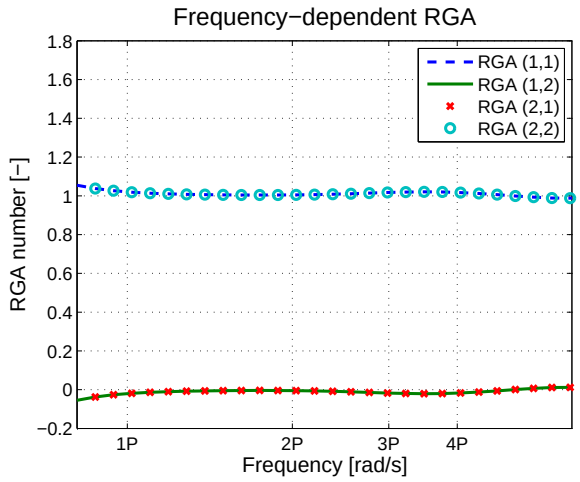

Figure 1. Relative Gain Array (RGA) evaluated for the 1P to the 4P frequency. The plot shows that the interactions in the cross terms from pitch angles θ_i to blade loads M_j where $i \neq j$ are negligible. This means that the two are decoupled and a decentralized control implementation is justified.

plementation after optimization. Optimization results of the feedforward IPC controller are given for the below and above-rated region, but a performance comparison is only presented for the above-rated region, as IPC for blade fatigue load reductions is generally only active in this operating region. An assumption is the availability of a rotor effective wind speed estimate [18] or measurement by e.g., a LIght Detection And Ranging (LIDAR) device [19].

To justify a decentralized feedforward control implementation, a linear model from blade pitch angles θ_i to harmonic blade loads M_j is identified to reveal the level of interaction using a frequency-dependent Relative Gain Array (RGA) [20]. It is confirmed in Figure 1 that interactions between both blades are negligible around the once- and twice-per-revolution (1P, 2P) periodic loads.

Assume the wind turbine system given by

$$\begin{bmatrix} M_1 \\ M_2 \end{bmatrix} = G_0 \begin{bmatrix} \theta_1 \\ \theta_2 \end{bmatrix} + \begin{bmatrix} v_1 \\ v_2 \end{bmatrix}, \tag{1}$$

where G_0 is a control oriented Multiple-Input Multiple-Output (MIMO) (non-)linear wind turbine model with blade pitch angles θ_i as input, blade load measurements M_j as output and v_k represents blade load disturbances originating from wind, caused by wind shear, tower shadow, upflow and shaft-tilt [18].

A decoupled fixed-structure feedforward IPC controller generating independent blade pitch signals to attenuate the above-mentioned disturbances is proposed. The feedforward controller that will be optimized for 1P and 2P periodic blade load reductions with respect to a predefined cost function is

$$\boldsymbol{C}(\psi, \boldsymbol{P}_i(u)) = \begin{cases} \theta_1(\psi, \boldsymbol{\rho}_{i,\theta_1}(u)) = \rho_{i,1}\sin(\psi) + \rho_{i,2}\cos(\psi) + \rho_{i,3}\sin(2\psi) + \rho_{i,4}\cos(2\psi) & \text{(2a)} \\ \theta_2(\psi, \boldsymbol{\rho}_{i,\theta_2}(u)) = \rho_{i,5}\sin(\psi) + \rho_{i,6}\cos(\psi) + \rho_{i,7}\sin(2\psi) + \rho_{i,8}\cos(2\psi), & \text{(2b)} \end{cases}$$

where ψ is the rotor azimuth angle. The control parameters $\rho_{i,j}$ are collected in the control parameter vector $\boldsymbol{P}_i(u) = \left[\boldsymbol{\rho}_{i,\theta_1}(u)\ \boldsymbol{\rho}_{i,\theta_2}(u)\right]$, where the iteration number is indicated by i, but is omitted when the variable is implied. As will be shown later, the control parameters depend on the wind speed u, and should be scheduled on an estimate or measurement accordingly. For

ease of notation, the argument u will be omitted in the sequel of this paper.

The feedforward control law defined in (2), consists of a weighted linear combination of sines and cosines. The summation of a sine and cosine at the same frequency, represent a sinusoidal function at that frequency with an amplitude and phase shift [21], such that

$$a\sin(n\psi) + b\cos(n\psi) = c\sin(n\psi + \phi) \quad \text{where} \quad c = \sqrt{a^2 + b^2} \quad \text{and} \quad \phi = \text{atan2}(b, a), \tag{3}$$

where n is an integer representing the nP harmonic for which the controller is optimized. Note that feedback control will pick up all frequencies and therefore the actuator duty increases when turbulence is present. The feedforward approach is aimed to limit the actuator duty cycle, and to minimize periodic 1P and 2P fatigue loads on the blades of the two-bladed wind turbine by only including these harmonics in the pitch signals. The load minimization objective is expressed in the cost function

$$J(\boldsymbol{P}_i) = \frac{1}{2N}\sum_{t=1}^{N}\left[\tilde{M}_1(t, \boldsymbol{\rho}_{i,\theta_1})^2 + \tilde{M}_2(t, \boldsymbol{\rho}_{i,\theta_2})^2\right], \tag{4}$$

where $\tilde{M}_j$ represents a bandpass filtered blade root bending moment signal around the 1P and 2P frequencies, and N the amount of samples in the data set. The gradient of the cost function with respect to the control parameters $\partial J/\partial \boldsymbol{P}(\boldsymbol{P}_i)$ is given by

$$\frac{\partial J}{\partial \boldsymbol{P}}(\boldsymbol{P}_i) = \frac{1}{N}\sum_{t=1}^{N}\left[\tilde{M}_1(t, \boldsymbol{\rho}_{i,\theta_1})\frac{\partial \tilde{M}_1}{\partial \boldsymbol{P}}(t, \boldsymbol{\rho}_{i,\theta_1})^T + \tilde{M}_2(t, \boldsymbol{\rho}_{i,\theta_2})\frac{\partial \tilde{M}_2}{\partial \boldsymbol{P}}(t, \boldsymbol{\rho}_{i,\theta_2})^T\right] \tag{5}$$

$$= \frac{1}{N}\sum_{t=1}^{N}\left[\tilde{M}_1(t, \boldsymbol{\rho}_{i,\theta_1})\frac{\partial \tilde{M}_1}{\partial \boldsymbol{\rho}_{\theta_1}}(t, \boldsymbol{\rho}_{i,\theta_1}) \quad \tilde{M}_2(t, \boldsymbol{\rho}_{i,\theta_2})\frac{\partial \tilde{M}_2}{\partial \boldsymbol{\rho}_{\theta_2}}(t, \boldsymbol{\rho}_{i,\theta_2})\right]^T, \tag{6}$$

which has to be obtained in each iteration for the control parameter update algorithm, and requires normal blade load measurement data $\tilde{\boldsymbol{M}}(t, \boldsymbol{P}_i)$ and its gradient $\partial \tilde{\boldsymbol{M}}/\partial \boldsymbol{P}(t, \boldsymbol{P}_i)$.

The approach for collecting the blade root moment signals and their gradients with respect to the control parameters is visualized in Figure 2, and respectively defined in Equation (1) and the following gradient output equation

$$\frac{\partial \boldsymbol{M}}{\partial \boldsymbol{P}}(t, \boldsymbol{P}_i) = \begin{bmatrix} \frac{\partial M_1}{\partial \boldsymbol{\rho}_{\theta_1}}(t, \boldsymbol{\rho}_{i,\theta_1}) \\ \frac{\partial M_2}{\partial \boldsymbol{\rho}_{\theta_2}}(t, \boldsymbol{\rho}_{i,\theta_2}) \end{bmatrix} = G_0 \begin{bmatrix} \frac{\partial \theta_1}{\partial \boldsymbol{\rho}_{\theta_1}}(\psi, \boldsymbol{\rho}_{i,\theta_1}) \\ \frac{\partial \theta_2}{\partial \boldsymbol{\rho}_{\theta_2}}(\psi, \boldsymbol{\rho}_{i,\theta_2}) \end{bmatrix} + \begin{bmatrix} v_1 \\ v_2 \end{bmatrix}, \tag{7}$$

where the signals are bandpass-filtered around the 1P and 2P frequency, denoted by a tilde $\tilde{(\cdot)}$. Bandpass filtering the blade load signals is done offline as part of the controller update iteration by a Finite Impulse Response (FIR) filter, to obtain a zero-phase shifted signal [22]. It is also possible to use a lower order Infinite Impulse Response (IIR) filter online. The two signals consist of an equal number of samples N and data collection is in both cases started at a (near) equal rotor azimuth angle. The amount of samples required for each individual experiment is specified in Section 3, and depends on the amount of turbulence and sensor noise present.

To end up with an unbiased estimate of the cost function gradient $\partial J/\partial \boldsymbol{P}(\boldsymbol{P}_i)$, independent normal and gradient experiments need to be performed under similar environmental conditions, as visualized in Figure 2. In [12], a method is described where only one gradient experiment is

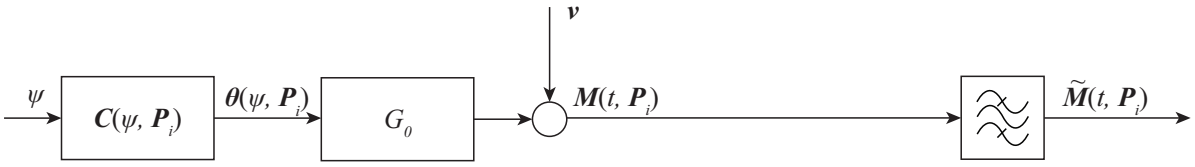

(a) Normal experiment for obtaining $\tilde{\boldsymbol{M}}(t, \boldsymbol{P}_i)$

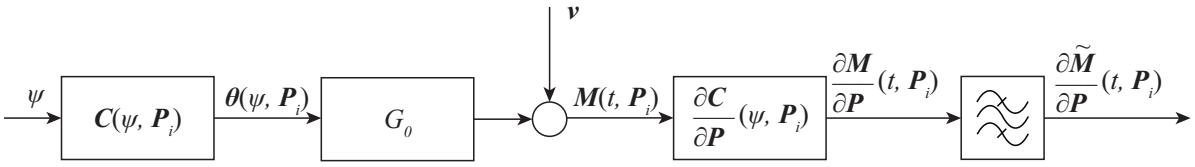

(b) Gradient experiment for obtaining $\partial\tilde{\boldsymbol{M}}/\partial\boldsymbol{P}(t, \boldsymbol{P}_i)$

Figure 2. Visualizations of experiments that need to be performed to obtain an estimate of the cost function gradient $\partial J/\partial \boldsymbol{P}(\boldsymbol{P}_i)$. The last symbol represents a bandpass-filter around the 1P and 2P frequency.

needed to generate the gradient $\partial\tilde{\boldsymbol{M}}/\partial\boldsymbol{P}(t, \boldsymbol{P}_i)$. Instead of using the controller gradient with respect to each individual parameter as an input to the system, the output is filtered through the gradient array of the controller with respect to all its parameters. This method is employed for optimization of the feedforward controller: during the gradient experiment, the blade load signal is filtered through an array of partial derivatives of the controller with respect to the control parameters in $\boldsymbol{P}$. Now, with the required signals at hand, an update of the control parameters can be computed by a Gauss-Newton based scheme

$$\boldsymbol{P}_{i+1} = \boldsymbol{P}_i - \gamma_i \boldsymbol{R}_i^{-1} \frac{\partial J}{\partial \boldsymbol{P}}(\boldsymbol{P}_i), \tag{8}$$

where γ_i is the algorithm step size and $\boldsymbol{R}_i$ is an approximation of the Hessian of $\tilde{\boldsymbol{M}}$ [13], which is given by

$$\boldsymbol{R}_i = \frac{1}{N} \sum_{t=1}^{N} \frac{\partial\tilde{\boldsymbol{M}}}{\partial\boldsymbol{P}}(t, \boldsymbol{P}_i) \frac{\partial\tilde{\boldsymbol{M}}}{\partial\boldsymbol{P}}(t, \boldsymbol{P}_i)^T. \tag{9}$$

The Hessian could also be simply chosen as an identity matrix I of appropriate size, but this would in general greatly deteriorate the convergence speed of the algorithm. Another option to reduce the amount of iterations by improving convergence speed is to include one additional experiment to obtain an extra set of the gradient $\partial\tilde{\boldsymbol{M}}/\partial\boldsymbol{P}(t, \boldsymbol{P}_i)$ [23], such that an unbiased estimate of the Hessian can be computed. In this work the Hessian as defined in Equation (9) is used, as the influence on convergence speed appeared to be minimal.

3. Results

The above described method is implemented in the high-fidelity wind turbine simulation software `GH BLADED` [24] by linking the algorithm designed in `MATLAB/Simulink` [25] to the external controller interface, using a model of the two-bladed 6 MW 2B6 wind turbine from 2-B Energy [2]. The sampling time T_s is set to 0.02 s. Optimizations of the feedforward controller are performed under ideal constant and under realistic turbulent wind conditions, collecting $N = 5000$ and $N = 12500$ data samples per experiment respectively, for wind speeds from 4 to 22 m/s. For

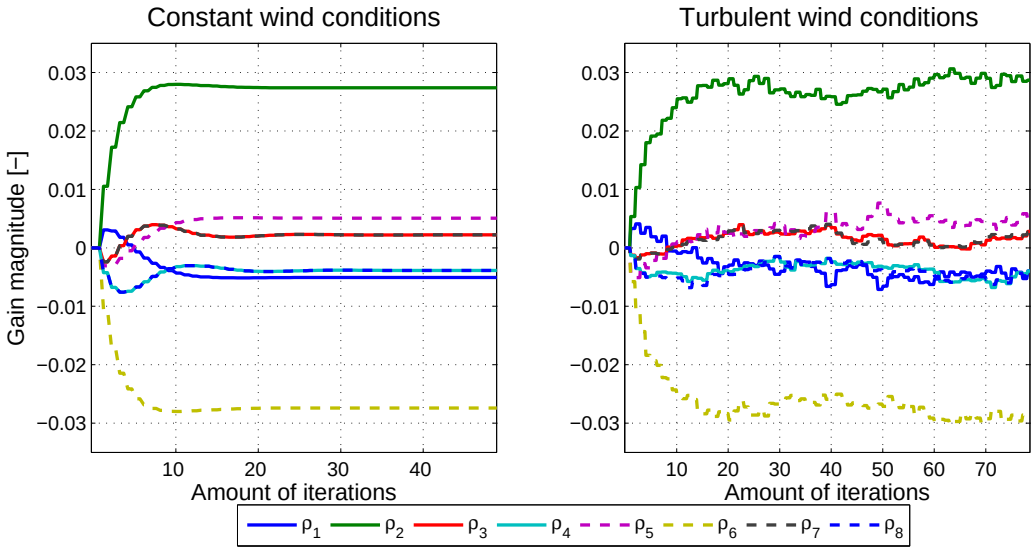

Figure 3. Optimization progress of the control parameters in $\boldsymbol{P}$ for 1P/2P harmonic load reductions during constant and turbulent 20 m/s wind conditions (15 % turbulence intensity).

all cases involving turbulent wind, a turbulence intensity of 15 % is used. For all optimizations, the initial control parameter vector $\boldsymbol{P}_0$ is set to the zero vector, meaning there is no IPC active initially, and the parameter search space is chosen to be unbounded.

Optimizations are performed for below and above-rated wind speeds from 4 to 22 m/s. In Figure 3, the convergence of the control parameters in $\boldsymbol{P}$ is presented. In constant wind conditions (left plot), the algorithm converges to the optimal parameters with the highest blade load reduction capabilities, which results in a signal equal to the one generated by feedback IPC. In turbulent conditions (right plot), the algorithm converges to a set of control parameters, minimizing blade fatigue loads on average. Because the optimized controller generates pitch

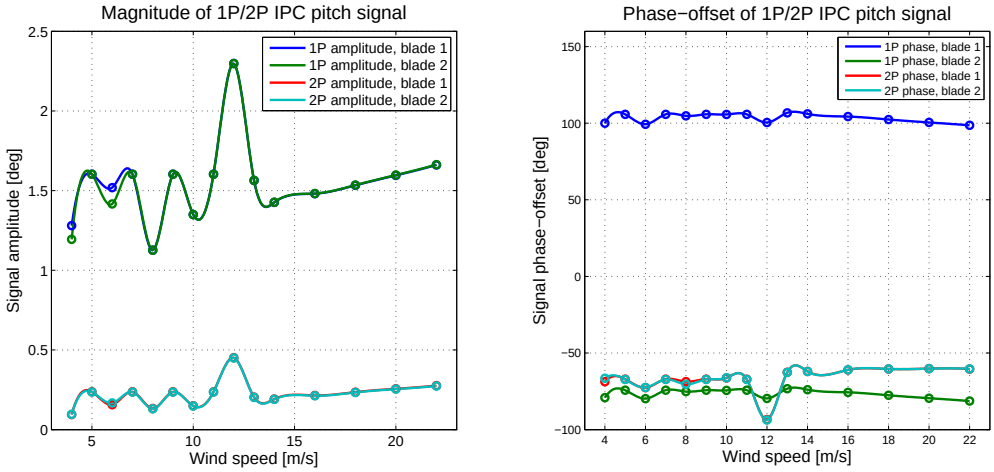

Figure 4. Amplitude a and phase ϕ for the 1P and 2P components of the optimal pitch signal represented as $a \sin(n\psi + \phi)$, evaluated at below and above-rated wind speeds, from 4 to 22 m/s.

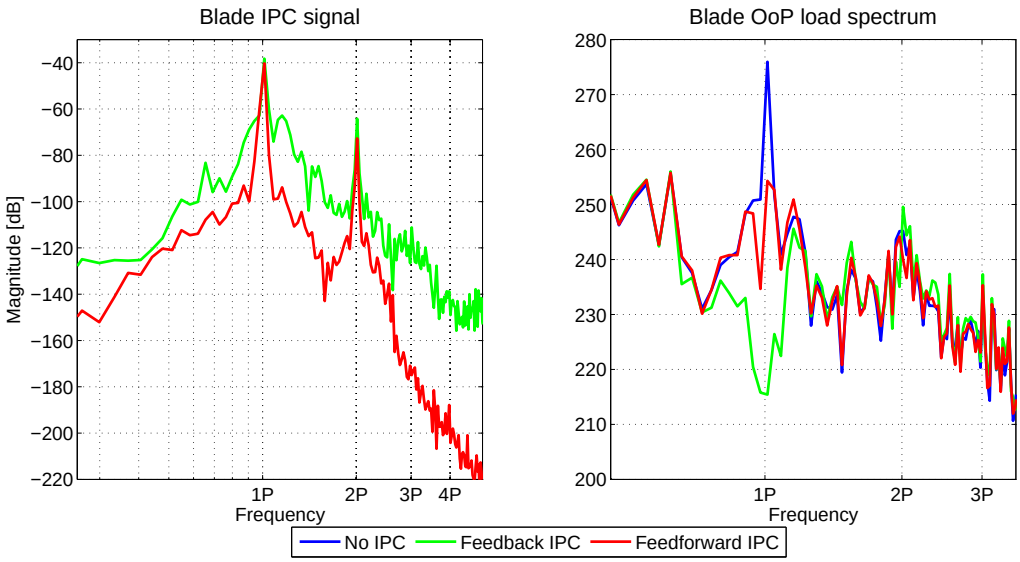

Figure 5. Pitch signal and blade load spectra with feedforward and feedback IPC and without IPC compared (1P/2P), under turbulent 20 m/s wind conditions (15 % turbulence intensity).

signals with a fixed amplitude and phase for each wind speed, and only uses the rotor azimuth angle after optimization, fatigue loads will be minimized on average as the feedforward controller does not respond to instantaneous load fluctuations. It is observed that the control parameter vector $\boldsymbol{P}$ in the turbulent case, converges to the values found after optimization in constant wind conditions. For this reason, the controller found in the latter case will be used during evaluation of its performance in both constant and turbulent wind conditions. Considering the observations described above, it is assumed that the found minimum represent the global minimum of the load minimization optimization problem.

An overview of the amplitude a and phase ϕ (see Equation (3)) of the optimized feedforward IPC signals as in a regular sinusoid $a \sin(n\psi + \phi)$ at the previously defined wind speeds, is given in Figure 4. The results shown are obtained after optimization under constant wind conditions. In the below-rated region, it is noted that the signal minimizing blade loads varies significantly in terms of amplitude but not in phase. In the cross-over region from below to above-rated conditions around a wind speed of 12 m/s, a large pitch signal amplitude is observed, which is probably an effect of the high thrust force acting on the turbine at the end of the below-rated region. In the above-rated region, the pitch signal amplitude is affine with respect to increasing wind speeds.

Figure 5 shows the pitch signal spectra of both feedforward and feedback IPC, as well as the blade load spectra in the case with feedforward and feedback IPC and without IPC in turbulent wind conditions. In the left plot it can be seen that both the feedforward and feedback controllers are active at the 1P and 2P frequencies, though the feedforward controller operates in a smaller frequency range around the nP harmonics resulting in a lower actuator duty cycle. The right plot shows that although the feedback controller is more successful in reducing the 1P harmonic load, both controllers significantly reduce the first harmonic load. The effect on 2P harmonic load reduction of both controllers is minimal. Because the feedforward controller is iteratively optimized on blade load measurement data sets of length N, particularly the deterministic periodic blade loads are reduced. Figure 6, where blade and rotating hub $M_{x,y}$ DELs in

case of feedforward and feedback IPC are compared against the case without IPC, shows similar results. Feedforward IPC significantly reduces the M_y blade and rotating hub DELs, while a slight increase in M_x DELs is observed. Compared to feedforward IPC, feedback IPC is able to reduce the M_y DELs even further.

Finally, a time-domain plot of the pitch signals generated by the feedforward and feedback control set-up is presented in Figure 7. This plot shows that the feedback IPC signal alternately leads and lags in time compared to the feedforward pitch signal, which is only a function of the rotor azimuth angle. This observation leads to the conclusion that feedback IPC is able to react to blade load intensity variations to actively follow and reduce the nP load, which explains its higher load reduction capabilities, but at cost of increased duty cycle of the pitch actuators. A cumulative sum of the total traveled angle of the feedforward IPC method compared to the feedback case shows a decrease of 13 %.

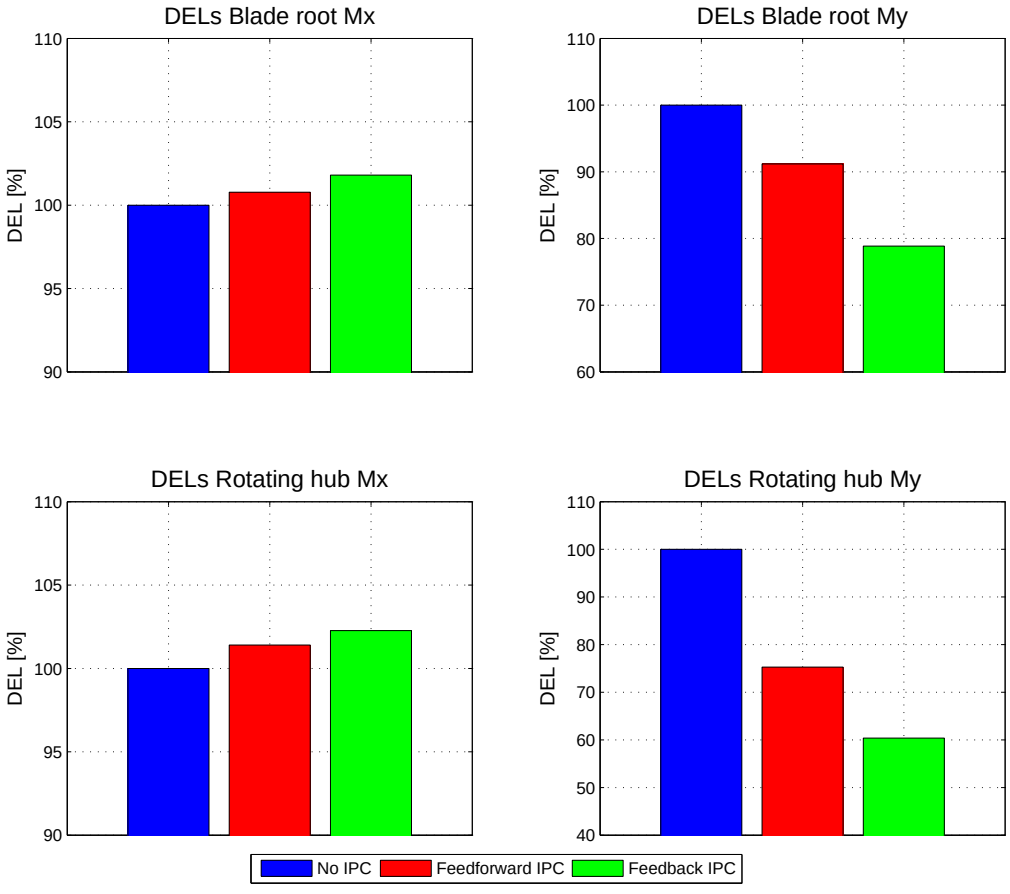

Figure 6. Blade and rotating hub $M_{x,y}$ DELs for feedforward and feedback IPC compared to the case without IPC, where the latter mentioned is set to 100 %, under turbulent 20 m/s wind conditions (15 % turbulence intensity).

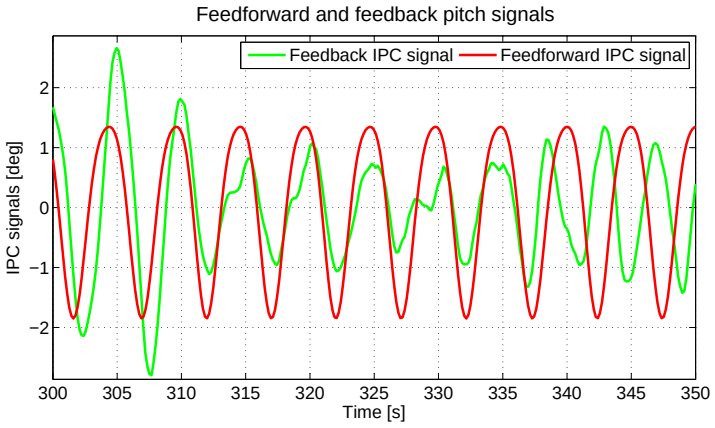

Figure 7. Feedforward and feedback pitch signal compared. The feedback pitch signal leads and lags in phase with respect to the feedforward pitch signal, as it depends on both blade load and rotor azimuth angle measurement signals.

4. Conclusion

A self-optimizing iterative update scheme for feedforward IPC is proposed. The approach is able to optimize a feedforward IPC controller for blade fatigue load reductions, based on blade root moment measurement signals. The iterative optimization scheme performs well in constant wind conditions for all wind speeds, and the load reduction capabilities matches with the feedback control implementation. The algorithm is able to optimize the feedforward controller in the above-rated region for turbulent and non-turbulent wind conditions. While conventional feedback IPC is still superior in terms of blade load reduction capabilities, the feedforward implementation alleviates periodic blade loads considerably with a perfect sinusoidal and reduced amplitude pitch signal. Pitch signal spectra show reduced activity around the 1P and 2P harmonics, which could extend the actuator lifetime. Because the feedforward controller only uses the rotor azimuth angle and a wind speed estimate or measurement after optimization on blade load data, it is possible to reduce the dependency on blade load measurements (i.e. remove redundant blade moment sensors) or to only temporarily apply blade load sensors during commissioning of the wind turbine for tuning purposes.

Acknowledgments

The work in this paper is supported by 2-B Energy. Their cooperation is hereby gratefully acknowledged.

References

[1] TKI Wind op Zee 2015 Cost reduction options for Offshore wind in the Netherlands FID 2010-2020
[2] 2-B Energy - Offshore Wind Turbine Devolopment. Website: `http://www.2benergy.com`, 2014
[3] Diepeveen NFB 2013 On the application of fluid power transmission in offshore wind turbines *TU Delft, Delft University of Technology*
[4] Schorbach V and Dalhoff P 2012 Two bladed wind turbines: antiquated or supposed to be resurrected? *Proc. of the EWEA Conf.*
[5] Van Solingen E, Beerens J, Mulders SP, De Breuker R and Van Wingerden JW 2016 Control design for a two-bladed downwind teeterless damped free-yaw wind turbine *Mechatronics* **36**: 77-96
[6] Bir G 2008 Multiblade coordinate transformation and its application to wind turbine analysis *ASME Wind Energy Symp.*
[7] Van Solingen E and Van Wingerden JW 2015 Linear individual pitch control design for two-bladed wind turbines *Wind Energy* **18.4**: 677-697
[8] Johnson W 2012 Helicopter theory *Courier Corporation*
[9] Park RH 1929 Two-reaction theory of synchronous machines generalized method of analysis-part I *Transactions of the American Institute of Electrical Engineers* **48.3**: 716-727
[10] Bossanyi EA 2003 Individual blade pitch control for load reduction *Wind energy* **6.2**: 119-128
[11] Navalkar ST, Van Wingerden JW, Van Solingen E, Oomen T, Pasterkamp E and Van Kuik GAM 2014

Subspace predictive repetitive control to mitigate periodic loads on large scale wind turbines *Mechatronics* **24.8**: 916-925
[12] Hjalmarsson H et al 1998 Iterative feedback tuning: theory and applications *Control Systems* IEEE **18.4**: 26-41
[13] Hjalmarsson H 2002 Iterative feedback tuningan overview *Int. J. of adaptive control and signal processing* **16.5**: 373-95.
[14] Hjalmarsson H, Gunnarsson S and Gevers M 1994 A Convergent Iterative Restricted Complexity Control Design Scheme *Proceedings of the 33rd IEEE Conf. on Decision and Control* **2**: 1735-1740
[15] Van Solingen E and Van Wingerden JW 2016 Iterative feedback tuning of wind turbine controllers *Wind Energ Sci. Discuss.* Manuscript under review for journal Wind Energ. Sci.
[16] Stearns H, Mishra S and Tomizuka M 2008 Iterative tuning of feedforward controller with force ripple compensation for wafer stage *AMC'08. 10th IEEE International Workshop on Adv. Motion Control* 234-239
[17] Boeren F, Oomen T and Steinbuch M 2015 Iterative motion feedforward tuning: A data-driven approach based on instrumental variable identification *Control Engineering Practice* **37**: 11-19
[18] Bossanyi EA 2000 The design of closed loop controllers for wind turbines *Wind energy* **3-3**: 149-163
[19] Harris M, Hand M and Wright A 2006 *LIDAR for turbine control. NREL Technical Report* **NREL/TP-500-39154**
[20] Skogestad S and Postlethwaite I 2007 Multivariable Feedback Control: Analysis and Design *Wiley*
[21] Cazelais G Website: `http://pages.pacificcoast.net/~cazelais/252/lc-trig.pdf`, Accessed March 2016
[22] Kamen E and Heck BS 2007 Fundamentals of Signals and Systems Using the Web and MATLAB
[23] Solari G and Gevers M 2004 Unbiased estimation of the Hessian for iterative feedback tuning (IFT) *43rd IEEE Conf. on Decision and Control, 2004. CDC.* **2**: 1759-1760
[24] Garrad Hassan, Bladed 4.20, Website: `http://www.gl-garradhassan.com`, Accessed March 2016
[25] Mathworks, Simulink. Website: `http://www.mathworks.com`, Accessed March 2016